Age-Related Differences in the Choroid Plexus Structural Integrity Are Associated with Changes in Cognition

Zhaoyuan Gong[1*], Angelique de Rouen[1], Nathan Zhang[1], Joseph S.R. Alisch[1], Murat Bilgel[2], Yang An[2], Jonghyun Bae[1], Noam Y. Fox[1], Alex Guo[1], Susan M. Resnick[2], Caio Mazucanti[1], Samuel Klistorner[3], Alexander Klistorner[3], Josephine M. Egan[1], Mustapha Bouhrara[1*]

[1]Laboratory of Clinical Investigation, National Institute on Aging, National Institutes of Health, Baltimore, MD 21224, USA

[2] Laboratory of Behavioral Neuroscience, National Institute on Aging, National Institutes of Health, Baltimore, MD 21224, USA

[3] Save Sight Institute, Sydney Medical School, University of Sydney, Sydney, New South Wales, Australia

***Correspondence**

Zhaoyuan Gong, PhD. National Institute on Aging, NIH, Baltimore, 21224 MD, USA. zhaoyuan.gong@nih.gov

Mustapha Bouhrara, PhD. National Institute on Aging, NIH, Baltimore, 21224 MD, USA. bouhraram@mail.nih.gov

Abstract

The choroid plexus (CP) plays a critical role in maintaining central nervous system (CNS) homeostasis, producing cerebrospinal fluid, and regulating the entry of specific substances into the CNS from blood. CP dysfunction has been implicated in various neurological and psychiatric disorders, including Alzheimer's disease, Parkinson's disease, and multiple sclerosis. This study investigates the relationship between CP structural integrity and cognitive decline in normative aging, using structural and advanced magnetic resonance imaging techniques, including CP volume, diffusion tensor imaging indices (mean diffusivity, MD, and fractional anisotropy, FA) and relaxometry metrics (longitudinal, T_1, and transverse, T_2, relaxation times). Our results show that diminished CP microstructural integrity, as reflected by higher T_1, T_2, and MD values, or lower FA values, is associated with lower cognitive performance in processing speed and fluency. Notably, CP microstructural measures demonstrated greater sensitivity to cognitive decline than macrostructural measures, i.e. CP volume. Longitudinal analysis revealed that individuals with reduced CP structural integrity exhibit steeper cognitive decline over time. Furthermore, structural equation modeling revealed that a latent variable representing CP integrity predicts faster overall cognitive decline, with an effect size comparable to that of age. These findings highlight the importance of CP integrity in maintaining cognitive health and suggest that a holistic approach to assessing CP integrity could serve as a sensitive biomarker for early detection of cognitive decline. Further research is needed to elucidate the mechanisms underlying the relationship between CP structural integrity and cognitive decline and to explore the potential therapeutic implications of targeting CP function to prevent or treat age-related cognitive deficits.

Introduction

The choroid plexus (CP), a highly vascularized structure within the brain ventricles, is responsible for producing cerebrospinal fluid (CSF) by specialized epithelial cells. This process maintains the optimal composition and volume of CSF, providing essential cushioning and protection for the central nervous system (CNS) (1, 2). It also acts as a selective barrier between the blood and CSF, regulating the entry of substances into the CNS. Additionally, the CP structure facilitates bulk removal of waste products through the glymphatic system and plays pivotal roles in regulating chemical balance, ionic composition, immunosurveillance and influencing circadian rhythmicity (3-5). Dysregulation of these CNS processes can lead to cerebral tissue degeneration and neuroinflammatory responses, leading to disrupted neural signaling as well as concomitant cognitive impairments and motor dysfunction (6-8). Indeed, CP integrity is believed to play a significant role in cognition, as increasing research indicates that an enlarged CP is often associated with cognitive impairment in a myriad of conditions including mild cognitive impairment (9), Alzheimer's disease (AD) (10, 11), Parkinson's disease (PD) (12, 13), and multiple sclerosis (MS) (14, 15), where CP size correlates with the severity of cognitive decline. A larger CP may indicate a disruption in the brain's clearance system, potentially contributing to cognitive deficits (16, 17). Therefore, measuring macrostructural and microstructural changes of CP through advanced neuroimaging techniques - notably magnetic resonance imaging (MRI) - could potentially develop imaging biomarkers for early detection of cognitive decline. However, there is a paucity of research investigating the relationship between CP structural health and cognitive impairment in normative aging, particularly from a longitudinal perspective. Importantly, microstructural changes in the CP are likely to precede macrostructural changes (*i.e.*, volume changes) by decades, making it crucial to investigate microstructural alterations in relation to cognitive changes. Elucidating the role of the CP structural integrity in cognition could lead to the development of novel therapeutic strategies aimed at improving its function, offering promising avenues for early intervention and prevention of cognitive decline.

Established quantitative MRI (qMRI) techniques, including diffusion tensor imaging (DTI) metrics (mean diffusivity, MD, and fractional anisotropy, FA) and relaxometry indices (longitudinal relaxation time, T_1, and transverse relaxation time, T_2), enable assessment of differences in CP microstructural integrity with aging, obesity, and markers of neuroinflammation

and AD pathology (18-22). DTI metrics offer a sensitive tool for monitoring CP changes in aging and elucidating the interplay between CP function, metabolic dysfunctions, and AD progression. DTI is sensitive to the underlying microarchitectural status of the CNS tissue and the degree and direction of water molecule mobility (23), and has been extensively used to study brain maturation and degeneration (24). Reduced FA is associated with structural degeneration, whereas an increase in MD reflects damage to cerebral tissue microstructural integrity with increased water mobility. Similarly, T_1 and T_2 both depend on macromolecular tissue composition, biochemistry and water mobility (25). Changes in T_1 or T_2 are directly associated with cerebral microstructural tissue changes, where higher values indicate advanced cerebral tissue deterioration (25). Notably, these associations between qMRI metrics and cerebral microstructural changes are also observed in CP (19), reinforcing the potential of qMRI for monitoring CP microstructural alterations. While studies using structural MRI have revealed that greater CP volume is inversely correlated with cognitive performance including in the AD continuum (9, 26), studies investigating microstructural differences in CP and cognition, as probed using DTI or relaxometry metrics, are lacking, including in normative aging. Yet, such investigations would further our understanding of the complex relationships between CP microstructure, function, and cognitive health (22).

This study aims to investigate the relationship between CP structural integrity, cognitive function, and aging, leveraging both structural and qMRI techniques. Specifically, we aim to examine CP microstructural differences associated with normative aging and longitudinal cognitive decline, clarify the link between CP microstructure and age-related cognitive health, and assess the utility of DTI and relaxometry metrics as biomarkers for early cognitive decline detection. This work advances our understanding of the complex interplay between CP structure and cognitive health.

Materials and methods

Participants

The MRI protocol received approval from the MedStar Research Institute and the National Institutes of Health (NIH) Intramural Ethics Committees. All examinations adhered to the standards set by the NIH Institutional Review Board. Study participants were recruited from the Baltimore Longitudinal Study of Aging (BLSA) and the Genetic and Epigenetic Signatures of Translational Aging Laboratory Testing (GESTALT) study (27, 28). Details regarding the study population, experimental design, and measurement protocols of BLSA and GESTALT have been described in previous publications (27, 28). The BLSA is a longitudinal cohort study initiated in 1958, conducted and funded by the National Institute on Aging (NIA) Intramural Research Program (IRP). The BLSA enrolls healthy, community-dwelling adults without major chronic conditions or functional impairments. Similarly, the GESTALT study, launched in 2015, is also conducted and funded by the NIA IRP, with virtually identical inclusion and exclusion criteria. Participants in both studies underwent evaluations at the NIA's clinical research unit, with exclusions based on metallic implants, neurological or medical disorders, and cognitive impairment, as assessed through a comprehensive battery of cognitive tests (29).

Magnetic Resonance Imaging (MRI)

For each participant, the imaging protocol for longitudinal and transverse relaxation times (T_1, T_2) and DTI metrics (FA and MD) consisted of:

T_1 and T_2 mapping (30-33): 3D spoiled gradient recalled echo (SPGR) images were acquired with flip angles (FAs) of [2 4 6 8 10 12 14 16 18 20]°, echo time (TE) of 1.37 ms, repetition time (TR) of 5 ms, and acquisition time of ~5 min. Additionally, 3D balanced steady-state free precession (bSSFP) images were acquired with FAs of [2 4 7 11 16 24 32 40 50 60]°, TE of 2.8 ms, TR of 5.8 ms, and acquisition time of ~6 min. To account for off-resonance effects, bSSFP images were acquired with radiofrequency excitation pulse phase increments of 0 or π (34). All SPGR and bSSFP images had an acquisition matrix of 150 × 130 × 94, voxel size of 1.6 mm × 1.6 mm × 1.6 mm. The double-angle method (DAM) was used to correct for excitation radiofrequency inhomogeneity (35). For this, two fast spin-echo images were acquired with FAs of 45° and 90°, TE of 102 ms, TR of 3000 ms, acquisition voxel size of 2.6 mm × 2.6 mm × 4 mm,

and acquisition time of ~4 min. All images were acquired with field of view (FoV) of 240 mm × 208 mm × 150 mm.

FA and MD mapping (24, 36): DTI protocol consisted of diffusion-weighted images (DWI) acquired with single-shot Echo Planar Imaging (EPI), TR of 10,000 ms, TE of 70 ms, two b-values of 0 and 700 s/mm^2, with the latter encoded in 32 directions. The acquisition matrix was 120 × 104 × 75, with voxel size of 2 mm × 2 mm × 2 mm, with FoV of 240 mm × 208 mm × 150 mm.

MRI scans were performed on a 3T whole-body Philips MRI system (Achieva, Philips Healthcare, Best, The Netherlands), utilizing the internal quadrature body coil for transmission and an eight-channel phased-array head coil for signal reception.

MRI processing

MRI processing and analysis details can be found in Reference (19). In brief, scalp and nonparenchymal regions were eliminated using FSL. CP volume was calculated using FreeSurfer for each participant. CP masks were thoroughly examined and corrected manually when needed. T_1 and T_2 mapping as well as FA and MD mapping, were performed using FSL and in-house MATLAB scripts. Mean T_1, T_2, FA, and MD values were extracted from the CP region of interest (ROI) using the CP mask from FreeSurfer.

Cognitive assessment

Cognitive domain scores were obtained for memory (California Verbal Learning Test (37) immediate and long-delay free recall), attention (Trail Making Test (38) Part A and Digit Span (39) Forward), executive function (Trail Making Test Part B and Digit Span Backward), verbal fluency (Category (40) and Letter Fluency (41)), and processing speed (Trail Making Test (38) Part A and Digit Symbol Substitution Test). To obtain domain scores, each test score was first converted to a z-score using the baseline mean and standard deviation, and these z-scores were averaged within each cognitive domain. Before computing the z-scores for Trail Making Test Parts A and B, the individual cognitive test scores (time to completion, in seconds) were log-transformed and negated so that higher z-scores indicated shorter time to completion.

Statistical analyses

We conducted three statistical analyses to assess the relationship between CP and cognition. All reported p-values in the main manuscript are adjusted for multiple comparisons across all regressions using the Benjamini & Hochberg procedure. Analyses were programmed in R 4.4.2, with lme4, lavaan, and tidyverse packages.

CP Structural Integrity vs. Cognition: To assess the cross-sectional relationship between CP structural integrity and cognition, we paired cognition scores with the closest MRI scan in time to create cross-sectional datasets. We then performed multiple linear regressions to evaluate the association between each MRI metric and cognitive domain, specified as:

$$\text{Cognition} \sim \beta_0 + \beta_{\text{MRI}} \times \text{MRI} + \beta_{\text{Age}} \times \text{Age} + \beta_{\text{Sex}} \times \text{Sex} + \beta_{\text{EDU}} \times \text{EDU} + \beta_{\text{Race}} \times \text{Race} + \epsilon. \quad (\text{Eq. } 1)$$

where Cognition represents one of five cognitive domains: processing speed (PS), memory (MEM), verbal fluency (FLU), executive function (EF), or attention (ATT). MRI metrics include CP volume (Vol), longitudinal relaxation time (T_1), transverse relaxation time (T_2), fractional anisotropy (FA), and mean diffusivity (MD). We observed collinearity between MRI metrics and Age, which weakened the significance of expected age-related cognitive declines. To address this, we regressed MRI metrics on covariates and replaced the original MRI values with their residuals. Covariates included Age (at the time of MRI), Sex (coded with male as the reference group), EDU (years of education), and Race (categorized as White, Black, or Other, with White as the reference group). All continuous variables were standardized for analysis.

CP Structural Integrity vs. Changes in Cognition: To investigate the relationship between CP integrity and longitudinal cognitive changes, we constructed longitudinal datasets by pairing repeated cognitive assessments with each participant's single MRI scan. The longitudinal dataset comprised 320 observations from 116 unique participants. We employed linear mixed-effects models:

$$\text{Cognition}_{ij} \sim \beta_0 + \beta_{\text{Time}} \times \text{Time}_{ij} + \beta_{\text{MRI}} \times \text{MRI}_i + \beta_{\text{Time}\times\text{MRI}} \times \text{Time}_{ij} \times \text{MRI}_i + \beta_{\text{Age}} \times \text{Age}_i + \beta_{\text{Sex}} \times \text{Sex}_i + \beta_{\text{EDU}} \times \text{EDU}_i + \beta_{\text{Race}} \times \text{Race}_i + \epsilon_{ij} + b_i, \quad (\text{Eq. } 2)$$

where Cognition_{ij} represents the cognitive score for subject i at time point j in PS, MEM, FLU, EF, or ATT. Time_{ij} is the Time-to-MRI calculated as the time difference between the time point j and the time at MRI scan for subject i. MRI_i denotes the MRI metric for subject i at the time of the

MRI scan. The interaction term $Time_{ij} \times MRI_i$ tests whether MRI metrics modulate the rate of cognitive change over time. b_i is the random intercept for subject i, and ϵ_{ij} is the residual error for subject i at time point j. Age_i , Sex_i , EDU_i, and $Race_i$ were included as covariates, as previously defined.

Overall CP Integrity and Overall Cognitive Function: We employed structural equation modeling (SEM) to investigate the relationships between latent constructs representing CP integrity and cognitive decline. SEM is a comprehensive statistical approach that facilitates the analysis of complex relationships involving both measured variables and unobserved constructs (latent variables). In this study, we opted to construct two comprehensive latent variables: CP Integrity (CPI) and Cognitive Function (CogFun). The CPI latent variable represents the unobservable overall structural integrity of the CP, inferred collectively from macrostructural and microstructural MRI measurements. In contrast, CogFun represents the unobservable overall rate of cognitive function changes, derived from all rates of change in the evaluated cognitive domains. By modeling these latent variables, we aimed to holistically assess the impact of CPI on overall cognitive function. The measurement model for CPI (exogenous latent variable) is defined as:

$$\mathrm{CPI} = \sim \lambda_{\mathrm{T_1}} \times \mathrm{T_1} + \lambda_{\mathrm{T_2}} \times \mathrm{T_2} + \lambda_{\mathrm{FA}} \times \mathrm{FA} + \lambda_{\mathrm{MD}} \times \mathrm{MD} + \lambda_{\mathrm{Vol}} \times \mathrm{Vol} + \epsilon, \quad (\mathrm{Eq.}\,3)$$

where λ represents factor loadings, and ϵ represents residual variance. Similarly, the measurement model for CogFun (endogenous latent variable) is defined as:

$$\mathrm{CogFun} = \sim \lambda_{\mathrm{MEM}} \times \mathrm{R_{MEM}} + \lambda_{\mathrm{ATT}} \times \mathrm{R_{ATT}} + \lambda_{\mathrm{EF}} \times \mathrm{R_{EF}} + \lambda_{\mathrm{FLU}} \times \mathrm{R_{FLU}} + \lambda_{\mathrm{PS}} \times \mathrm{R_{PS}} + \epsilon, \quad (\mathrm{Eq.}\,4)$$

where R_{MEM}, R_{ATT}, R_{EF}, R_{FLU}, R_{PS} are rates of change in memory, attention, executive function, fluency, and processing speed, respectively. We modeled the structural relationship between CP Integrity and cognitive function as:

$$\mathrm{CogFun} \sim \beta_{\mathrm{CPI}} \times \mathrm{CPI} + \beta_{\mathrm{Age}} \times \mathrm{Age} + \beta_{\mathrm{Sex}} \times \mathrm{Sex} + \beta_{\mathrm{EDU}} \times \mathrm{EDU} + \beta_{\mathrm{Race}} \times \mathrm{Race} + \epsilon. \quad (\mathrm{Eq.}\,5).$$

All results are presented in standardized form, with variables scaled to have a mean of zero and a standard deviation of one. This scaling allows parameter estimates (e.g., factor loadings, regression coefficients, and variances) to be interpreted as standardized effects.

Results

Table 1 provides an overview of the study demographics. A total of 116 unique subjects were included. In the cross-sectional cohort, the median time between cognitive testing and MRI scanning was 0 years (mean: -0.17 years; SD: 0.6 years). In the longitudinal cohort, participants underwent an average of 2.76 cognitive assessments (SD: 2.74), with a median follow-up duration of 5.3 years (mean: 8.8 years; SD: 7.9 years). The average age at the time of MRI scanning was 57.2 years, and 44.8% of the participants were female. The cohort's mean education level was 16.2 years (SD: 2.8 years). The cohort comprised 70.7% of white participants, indicating an imbalance in racial representation.

Figure 1 shows the results of the multiple linear regression analysis (Eq. 1) examining the cross-sectional relationship between each MRI metric (*i.e.*, CP volume, T_1, T_2, MD, and FA) and each cognitive domain (*i.e.*, PS, MEM, FLU, EF, and ATT). As expected, age was negatively associated with cognition in all examined regressions. These associations were all statistically significant. Examples of these associations are shown in Fig. 1B and C. Importantly, CP volume, T_1, T_2, and MD exhibited negative associations with cognition, while FA exhibited positive association with cognition, indicating that worse macrostructural CP integrity, represented by higher CP volume, and worse microstructural CP integrity, as measured by higher T_1, T_2, MD values and lower FA, are associated with worse cognition (Fig. 1D). However, these associations were statistically significant only for MD vs. FLU and PS as well as T_1, T_2, and FA vs. PS (Fig. 1D). Representative plots of these associations are shown in Fig. 1E and F. In addition, sex differences were significant, with males scoring higher in EF and ATT but lower in MEM. Higher education was significantly associated with better performance in MEM, FLU, EF, and ATT. White participants showed significantly better performance in ATT, EF, and PS. We note that the main purpose of this study is not to investigate the covariates, and the results may not be generalizable due to confounding factors. Complete analysis results are provided in the supplementary materials.

Figure 2 shows the results of the linear mixed-effects analysis (Eq. 2) examining the relationship between each MRI metric (*i.e.*, CP volume, T_1, T_2, MD, and FA) and longitudinal changes in each cognitive domain (*i.e.*, PS, MEM, FLU, EF, and ATT). Results are shown for the main parameters of interest relevant to this investigation, namely, MRI fixed effect, Time-to-MRI, and Time × MRI interaction. MRI metrics of CP volume, T_1, T_2, and MD exhibited negative associations with

cognition, while FA exhibited a positive association with cognition, indicating that worse CP structural integrity is associated with lower cognitive performance. These associations reached statistical significance for MD vs. PS, FLU and ATT as well as T_1, T_2 and FA vs. PS (Fig. 2A). Examples of plots of these associations are shown in Fig. 2B and C. Further, as expected, Time-to-MRI exhibited overall negative association with cognition, reaching significance in various pairwise MRI metrics vs. cognitive domains as indicated in Fig. 2D-F. Importantly, the association between Time × MRI interaction and cognition exhibited negative associations for Vol, T_1, T_2 and MD and positive associations for FA (Fig. 2G). These associations were statistically significant for several MRI metrics vs. cognitive domains (Fig. 2G). These analyses indicate that lower CP structural integrity, as reflected by higher CP volume, T_1, T_2 and MD values or lower FA values, is associated with steeper longitudinal decline in cognition. Fig.2 H and I show the example of higher T_1 value, corresponding to the value at the 75^{th} percentile marked with the green lines, is associated with steeper decline in PS and EF. Sex differences were significant, with males scoring higher in ATT but lower in MEM. Higher education was significantly associated with better performance in all cognitive domains, while White participants showed significantly better performance in ATT, EF, and PS. Same caution should be exercised for generalizing the results for covariates. Complete analysis results are provided in the supplementary materials.

Finally, Figure 3 shows the results of the SEM analysis investigating the relationship between combined MRI metrics (CPI) and combined change rates of cognitive function (CogFun) (Eqs. 3-5). As expected, derived rates of cognitive change exhibit decreased trends as a function of age, especially at older ages (Fig. 3A). Our analysis reveals that the measurement model for CP damage indicates significant standardized loadings for all MRI metrics. Interestingly, CP volume, a measure of macrostructural integrity, contributes the least to the latent variable as compared to all other MRI metrics, which are measures of microstructural alterations. Of note, FA exhibits a negative loading, as lower FA values reflect worse microstructural integrity. In the measurement model for cognitive changes, all rates of cognitive domain changes display significant loadings, with fluency contributing the least. The structural model reveals that CPI is negatively associated with CogFun ($\beta = -0.41$, $p < 0.001$), indicating that worse overall CP structural integrity predicts faster cognitive decline. This effect is close to that of age ($\beta = -0.55$, $p < 0.001$), highlighting a strong association. Furthermore, education exhibits a protective effect ($\beta = 0.28$, $p = 0.001$),

whereas the effects of sex ($\beta = -0.17$, $p = 0.045$) and race ($\beta = -0.06$, $p = 0.456$) are weaker, with the latter being nonsignificant.

Discussion

The present study revealed significant associations between CP integrity, as measured by MRI metrics, and cognitive function across various domains. Notably, our results showed that CP volume, T_1, T_2, and MD values were negatively correlated with cognitive performance, whereas FA values exhibited positive associations, indicating that compromised CP structural integrity is linked to poorer cognitive function. These findings were statistically significant for PS and FLU, suggesting that CP integrity plays a critical role in maintaining optimal cognitive performance. Furthermore, our analysis revealed that the associations between CP integrity and cognitive function were influenced by demographic factors, such as age, sex, education, and race, highlighting the importance of considering individual differences and sociological disparities related to demographic factors when examining the neural correlates of cognitive function. The observed relationships between CP integrity and cognitive decline also underscore the potential utility of MRI metrics as biomarkers for monitoring cognitive changes and detecting early signs of neurodegenerative diseases. Overall, our findings contribute to a deeper understanding of the complex interplay between brain structure and cognitive function and have significant implications for the development of novel diagnostic and therapeutic strategies aimed at promoting cognitive health and mitigating cognitive decline.

Existing evidence shows the sensitivity of microstructural changes to cognitive decline, which precedes macrostructural changes by decades (42, 43). By leveraging advanced MRI techniques, including diffusion and relaxometry, we demonstrate that microstructural alterations in the CP are more sensitive indicators of CP dysfunction and cognitive decline than macrostructural measurement. Previous research highlights the association between CP volume and cognitive impairment in various conditions. However, our study addresses a significant gap in the literature by investigating the relationship between CP microstructural integrity and cognitive decline in normative aging, using qMRI techniques. While previous studies have relied on structural MRI to examine the relationship between CP volume and cognitive performance (9, 10, 14, 44-47), our study provides novel insights into the microstructural changes underlying CP dysfunction and cognitive decline.

The mechanisms underlying the association between CP degeneration and cognitive decline are complex and multifaceted. Previous studies suggest that CP dysfunction may contribute

to cognitive decline through various pathways, including disrupted CSF dynamics (48-50), neuroinflammation (51-53), and impaired glymphatic function (54-56). The age-related increase in CP volume may lead to an inflammatory response at the blood/CP-CSF barrier as well as in the brain itself. Furthermore, the CP's role in regulating the entry of substances into the CNS and facilitating the removal of waste products from the brain may be compromised with aging (48, 49, 57, 58), leading to the accumulation of toxic substances and exacerbating cognitive decline. Additionally, the association between increased CP volume and impaired glymphatic function may also contribute to cognitive decline (54-56), as the glymphatic system plays a critical role in clearing metabolites from the brain. Further studies are needed to elucidate the underlying mechanisms and to determine the causal relationships between CP degeneration, neuroinflammation, and cognitive decline.

Although our study provides novel clinical insights into the relationship between CP structural integrity and cognitive decline in normative aging, some limitations should be acknowledged. First, our study employed a single time-point MRI assessment, which precludes the examination of longitudinal changes in CP structural integrity. Future studies incorporating longitudinal MRI assessments are necessary to verify the temporal relationships between CP structural changes and cognitive decline. Second, our study relied on indirect MRI markers of CP microstructural integrity, which cannot fully capture the complex cellular and molecular changes occurring within the CP. The development of more sensitive and specific biomarkers is needed to further elucidate the mechanisms underlying CP dysfunction and cognitive decline. Finally, our study did not control for potential confounding variables, such as sleep quality, physical activity, and social engagement, which may influence the relationship between CP microstructural integrity and cognitive decline. Future studies should strive to incorporate these variables to provide a more comprehensive understanding of the complex interplay between CP function, lifestyle factors, and cognitive health.

Conclusions

Our findings demonstrate that compromised CP structural integrity is significantly associated with cognitive decline in aging among cognitively unimpaired individuals. This underscores the importance of CP health in maintaining cognitive function and suggests that advanced CP imaging biomarkers could aid in early detection and intervention strategies for cognitive decline.

TABLE 1 Participant demographics for cross-sectional and longitudinal analysis

Characteristic	**Cross-sectional analysis (*N*=116)**	**Longitudinal analysis (*N*=116, N_{cog}=320)**
Age at MRI (years), mean (SD)	57.2 (20.9)	
Sex Female, n (%)	52 (44.8%)	
Education, mean (SD)	16.2 (2.8)	
Race, Black	22 (19%)	
White	82 (70.7%)	
API and Other	12 (10.3%)	
Number of cognitive assessments, mean (SD)	N/A	2.76 (2.74)
Duration of cognitive assessments (years), median (mean, SD)	N/A	5.3 (8.8, 7.9)

N, number of participants. N_{cog}, number of cognitive assessments. MRI, magnetic resonance imaging. API, Asian and Pacific Islander. SD, standard deviation.

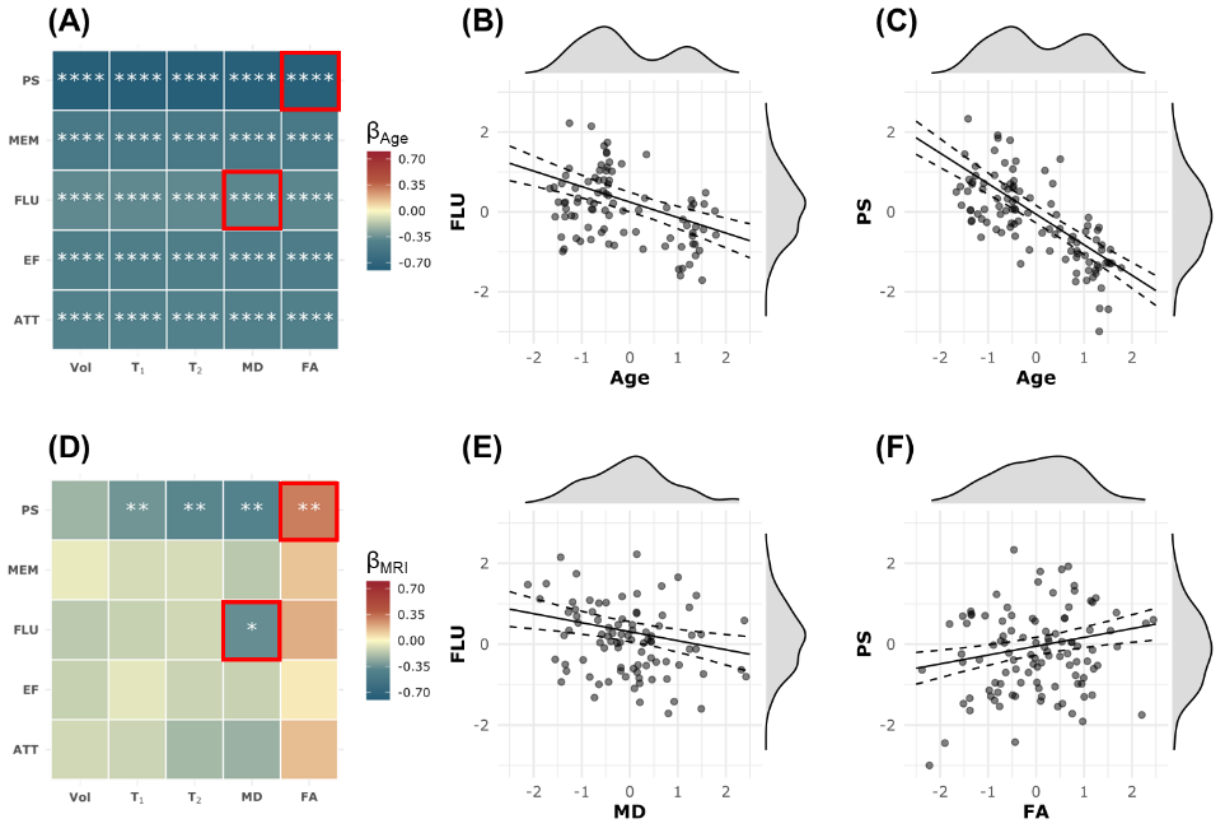

Figure 1. Pairwise multiple linear regression was conducted for each MRI metric and each cognitive domain. The explicit regression equation is: $Cognition \sim \beta_0 + \beta_{MRI} \times MRI + \beta_{Age} \times Age + \beta_{Sex} \times Sex + \beta_{EDU} \times EDU + \beta_{Race} \times Race + \epsilon$, *where Cognition includes processing speed (PS), memory (MEM), verbal fluency (FLU), executive function (EF), and attention (ATT). MRI metrics include the residuals of CP volume (Vol), T_1 relaxation time (T_1), T_2 relaxation time (T_2), fractional anisotropy (FA), and mean diffusivity (MD) after regressing with other covariates. All continuous variables are standardized.* ***Panels A and D*** *show the results for the regression coefficients of Age and MRI metrics, respectively. The estimated β coefficients are color-coded and statistically significant results are marked with asterisks, where * indicates $p < 0.05$, ** indicates $p < 0.01$, *** indicates $p < 0.001$, and **** indicates $p < 0.0001$. All p-values are corrected for multiple comparisons using the Benjamini–Hochberg (BH) procedure.* ***Panels B and E*** *present example results for the regression where the MRI metric is MD and the cognitive domain is FLU. There is a significant negative association between FLU and age (Panel B) and a significant negative association between MD and FLU (Panel E). High MD values indicate reduced microstructural integrity, which is associated with lower FLU.* ***Panels C and F*** *show*

example results for the regression where the MRI metric is FA and the cognitive domain is PS. In addition to a significant negative association between PS and age (Panel C), there is a significant positive association between FA and PS (Panel F). High FA values indicate greater microstructural integrity, which is associated with higher PS scores.

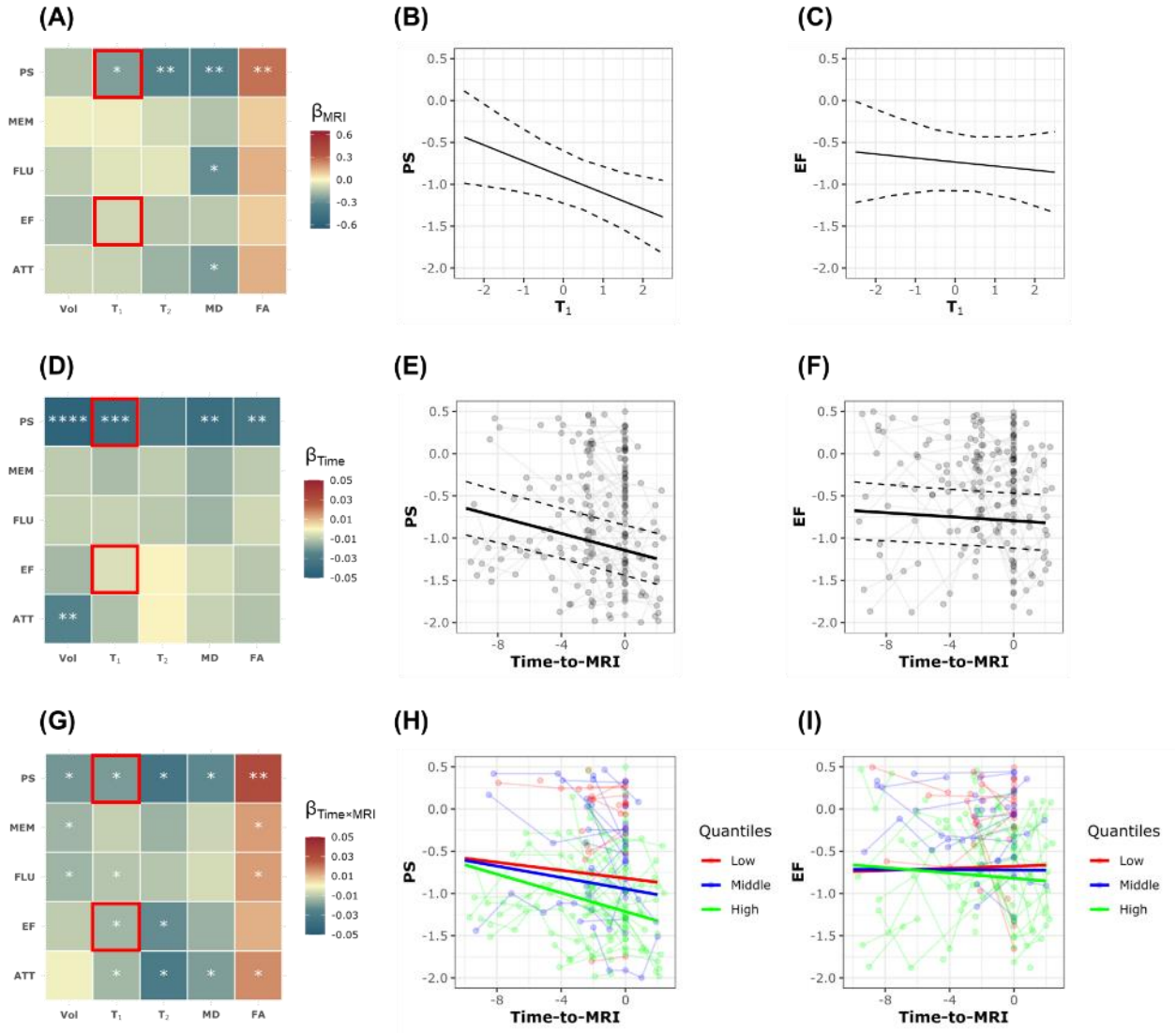

Figure 2. Pairwise linear mixed-effects (LME) models were conducted for each MRI metric and each cognitive domain. The explicit regression equation is: $Cognition_{ij} \sim \beta_0 + \beta_{Time} \times Time_{ij} + \beta_{MRI} \times MRI_i + \beta_{Time \times MRI} \times Time_{ij} \times MRI_i + \beta_{Age} \times Age_i + \beta_{Sex} \times Sex_i + \beta_{EDU} \times EDU_i + \beta_{Race} \times Race_i + \epsilon_{ij} + b_i$, *where* $Cognition_{ij}$ *includes longitudinal measurements of processing speed (PS), memory (MEM), verbal fluency (FLU), executive function (EF), and attention (ATT) for subject i at timepoint j.* $Time_{ij}$ *represents the time to the only MRI scan of subject i at timepoint j. MRI metrics (*MRI_i*) include CP volume (Vol),* T_1 *relaxation time (*T_1*),* T_2 *relaxation time (*T_2*), fractional anisotropy (FA), and mean diffusivity (MD) for subject i at the time of MRI scan. All continuous variables are standardized except for* $Time_{ij}$. ***Panels A, D and G*** *show the results for the regression coefficients of MRI metrics, Time and Time × MRI*

*interaction, respectively. The estimated β coefficients are color-coded and statistically significant results are marked with asterisks, where * indicates $p < 0.05$, ** indicates $p < 0.01$, *** indicates $p < 0.001$, and **** indicates $p < 0.0001$. All p-values are corrected for multiple comparisons using the Benjamini–Hochberg (BH) procedure.* ***Panels B, E, and H*** *present example results for the LME model where the MRI metric is T_1 and the cognitive domain is PS. A significant negative association between the fixed effect of T_1 and PS is observed (Panel B). This indicates that individuals with higher T_1 values tend to have consistently lower cognitive scores over time. PS also shows a significant linear decline over time (Panel E). Most importantly, the significant negative interaction term indicates that individuals with higher T_1 values experience faster declines in PS over time compared to those with lower T_1 values (green line vs. red line in Panel H).* ***Panels C, F, and I*** *present example results for the LME model where the MRI metric is T_1 and the cognitive domain is EF. No significant association is found between the fixed effect of T_1 and EF (Panel C). EF also does not show a significant general decline over time (Panel F). However, a significant negative interaction term is observed, indicating that individuals with higher T_1 values experience faster declines in EF over time compared to those with lower T_1 values (green line vs. red line in Panel I). Increased T_1 relaxation times could reflect microstructural changes such as reduced myelin integrity or axonal damage, which are known to impair cognitive processes and may exacerbate cognitive decline over time observed here.*

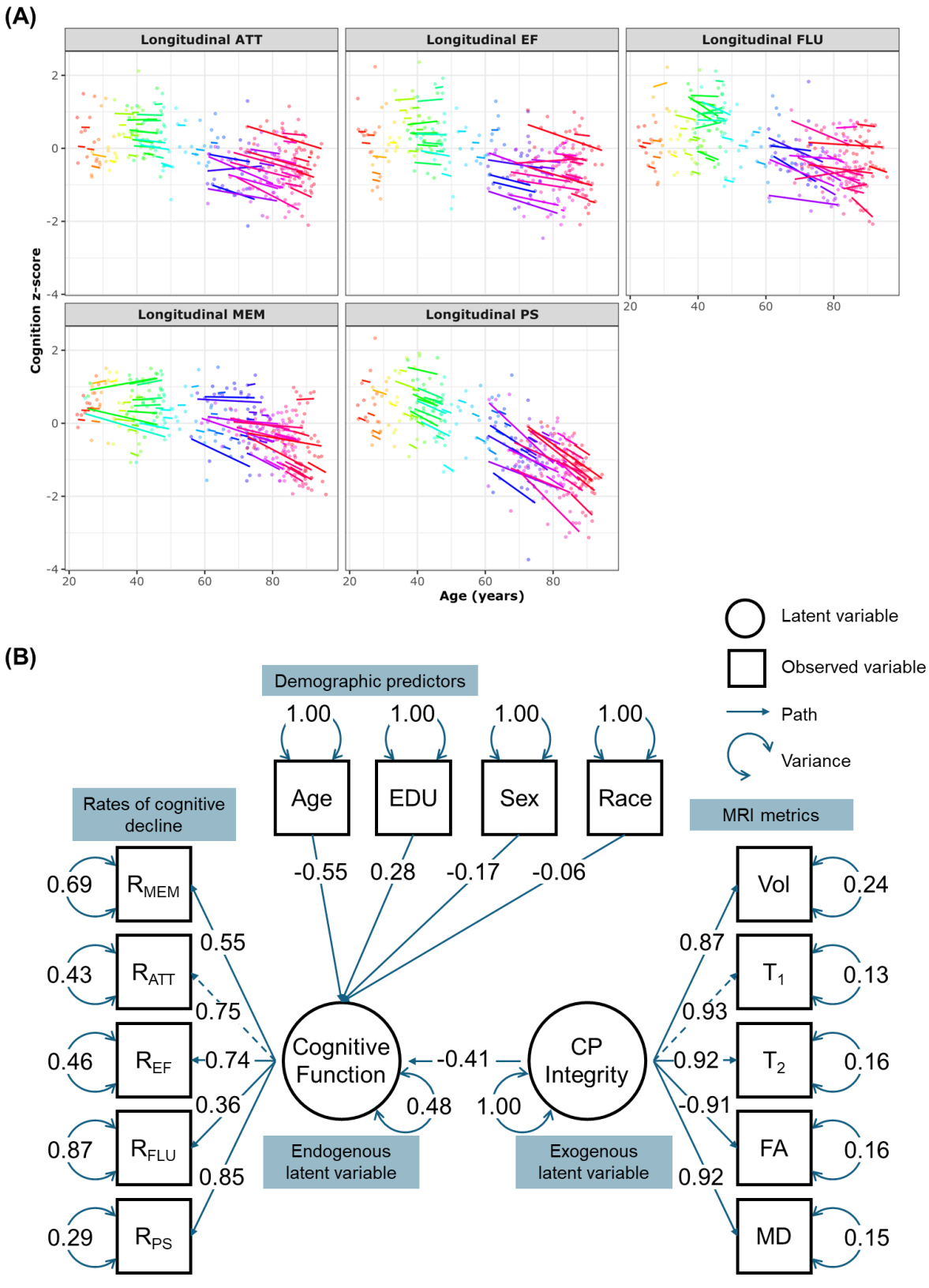

Figure 3. Structural equation modeling (SEM) was applied to investigate the relationship between combined MRI metrics (CPI) and combined rates of cognitive decline (CogFun). ***Panel A*** *displays the estimated rates of Cognitive-decline for each subject, derived from linear mixed-effects models:* $Cognition_{ij} \sim \beta_0 + \beta_{Time} \times Time_{ij} + b_{Time,i} \times Time_{ij} + \epsilon_{ij} + b_i$. *The rate of cognitive decline is defined as the sum of the fixed effect (β_{Time}) and the subject-specific random effect ($b_{Time,i}$). Each subject is color-coded and has a fitted decline line if more than two longitudinal measurements exist.* ***Panel B*** *visualizes the SEM results. The measurement model for CP integrity, CPI, (exogenous latent variable) is defined as:* $CPI = \sim \lambda_{T_1} \times T_1 + \lambda_{T_2} \times T_2 + \lambda_{FA} \times FA + \lambda_{MD} \times MD + \lambda_{Vol} \times Vol + \epsilon$, *where λ represents factor loadings, and ϵ represents residual variance. Similarly, the measurement model for Cognitive-function, Cog-Fun, (endogenous latent variable) is defined as:* $CogFun = \sim \lambda_{MEM} \times R_{MEM} + \lambda_{ATT} \times R_{ATT} + \lambda_{EF} \times R_{EF} + \lambda_{FLU} \times R_{FLU} + \lambda_{PS} \times R_{PS} + \epsilon$, *where R_{MEM}, R_{ATT}, R_{EF}, R_{FLU}, R_{PS} are rates of decline in memory, attention, executive function, fluency, and processing speed, respectively. The structural regression model is:* $CogFun \sim \beta_{CPI} \times CPI + \beta_{Age} \times Age + \beta_{Sex} \times Sex + \beta_{EDU} \times EDU + \beta_{Race} \times Race + \epsilon$. *The results are presented in the standardized form, allowing the parameter estimates to be interpreted as standardized effects. The measurement model for CPI indicates that all MRI metrics have significant standardized loadings, with CP volume contributing less to the latent variable because it reflects macrostructure, while other MRI metrics probe microstructure. Additionally, FA shows a negative loading because, unlike other MRI metrics, lower FA values indicate greater microstructural damage. In the measurement model for CogFun, all rates of cognitive domain changes have significant loadings, with fluency contributing the least. The structural model reveals that CPI has a significant negative effect on CogFun ($\beta = -0.41$, $p < 0.001$), suggesting that higher CPI predicts faster cognitive decline. This effect is comparable to that of age ($\beta = -0.55$, $p < 0.001$), indicating a strong association. Education ($\beta = 0.28$, $p = 0.001$) has a protective effect, while the effects of sex ($\beta = -0.17$, $p = 0.045$) and race ($\beta = -0.06$, $p = 0.456$) are weaker, with race being nonsignificant.*

Reference

1. Damkier HH, Brown PD, Praetorius J. Cerebrospinal Fluid Secretion by the Choroid Plexus. Physiological Reviews. 2013;93(4):1847-92.
2. Lun MP, Monuki ES, Lehtinen MK. Development and functions of the choroid plexus–cerebrospinal fluid system. Nature Reviews Neuroscience. 2015;16(8):445-57.
3. Talhada D, Costa-Brito AR, Duarte AC, Costa AR, Quintela T, Tomás J, et al. The choroid plexus: Simple structure, complex functions. Journal of Neuroscience Research. 2020;98(5):751-3.
4. Myung J, Schmal C, Hong S, Tsukizawa Y, Rose P, Zhang Y, et al. The choroid plexus is an important circadian clock component. Nature Communications. 2018;9(1):1062.
5. Quintela T, Furtado A, Duarte AC, Gonçalves I, Myung J, Santos CRA. The role of circadian rhythm in choroid plexus functions. Progress in Neurobiology. 2021;205:102129.
6. Gong Z, Bilgel M, Kiely M, Triebswetter C, Ferrucci L, Resnick SM, et al. Lower myelin content is associated with more rapid cognitive decline among cognitively unimpaired individuals. Alzheimers Dement. 2023;In Press.
7. Gong Z, Faulkner ME, Akhonda M, Guo A, Bae J, Laporte JP, et al. White matter integrity and motor function: a link between cerebral myelination and longitudinal changes in gait speed in aging. Geroscience. 2024.
8. Gong Z, Bilgel M, An Y, Bergeron CM, Bergeron J, Zukley L, et al. Cerebral white matter myelination is associated with longitudinal changes in processing speed across the adult lifespan. Brain Commun. 2024;6(6):fcae412.
9. Umemura Y, Watanabe K, Kasai S, Ide S, Ishimoto Y, Sasaki M, et al. Choroid plexus enlargement in mild cognitive impairment on MRI: a large cohort study. Eur Radiol. 2024;34(8):5297-304.
10. Jeong SH, Park CJ, Cha J, Kim SY, Lee SK, Kim YJ, et al. Choroid Plexus Volume, Amyloid Burden, and Cognition in the Alzheimer's Disease Continuum. Aging Dis. 2024.
11. Hong H, Hong LW, Luo X, Zeng QZ, Li KC, Wang SY, et al. The relationship between amyloid pathology, cerebral small vessel disease, glymphatic dysfunction, and cognition: a study based on Alzheimer's disease continuum participants. Alzheimers Res Ther. 2024;16(1).
12. Jeong SH, Jeong HJ, Sunwoo MK, Ahn SS, Lee SK, Lee PH, et al. Association between choroid plexus volume and cognition in Parkinson disease. Eur J Neurol. 2023;30(10):3114-23.
13. He P, Gao Y, Shi L, Li Y, Qiu Y, Feng S, et al. The association of CSF biomarkers and cognitive decline with choroid plexus volume in early Parkinson's disease. Parkinsonism Relat Disord. 2024;120:105987.
14. Preziosa P, Pagani E, Meani A, Storelli L, Margoni M, Yudin Y, et al. Chronic Active Lesions and Larger Choroid Plexus Explain Cognition and Fatigue in Multiple Sclerosis. Neurol Neuroimmunol Neuroinflamm. 2024;11(2):e200205.
15. Ricigliano VAG, Morena E, Colombi A, Tonietto M, Hamzaoui M, Poirion E, et al. Choroid Plexus Enlargement in Inflammatory Multiple Sclerosis: 3.0-T MRI and Translocator Protein PET Evaluation. Radiology. 2021;301(1):166-77.
16. Lizano P, Lutz O, Ling G, Lee AM, Eum S, Bishop JR, et al. Association of Choroid Plexus Enlargement With Cognitive, Inflammatory, and Structural Phenotypes Across the Psychosis Spectrum. Am J Psychiatry. 2019;176(7):564-72.
17. Umemura Y, Watanabe K, Kasai S, Ide S, Ishimoto Y, Sasaki M, et al. Choroid plexus enlargement in mild cognitive impairment on MRI: a large cohort study. European radiology. 2024;34(8):5297-304.
18. Alisch JSR, Egan JM, Bouhrara M. Differences in the choroid plexus volume and microstructure are associated with body adiposity. Front Endocrinol (Lausanne). 2022;13:984929.

19. Alisch JSR, Kiely M, Triebswetter C, Alsameen MH, Gong Z, Khattar N, et al. Characterization of Age-Related Differences in the Human Choroid Plexus Volume, Microstructural Integrity, and Blood Perfusion Using Multiparameter Magnetic Resonance Imaging. Front Aging Neurosci. 2021;13:734992.
20. Bouhrara M, Walker KA, JS RA, Gong Z, Mazucanti CH, Lewis A, et al. Association of Plasma Markers of Alzheimer's Disease, Neurodegeneration, and Neuroinflammation with the Choroid Plexus Integrity in Aging. Aging Dis. 2024.
21. Alicioglu B, Yilmaz G, Tosun O, Bulakbasi N. Diffusion-weighted magnetic resonance imaging in the assessment of choroid plexus aging. Neuroradiol J. 2017;30(5):490-5.
22. Hong H, Hong L, Luo X, Zeng Q, Li K, Wang S, et al. The relationship between amyloid pathology, cerebral small vessel disease, glymphatic dysfunction, and cognition: a study based on Alzheimer's disease continuum participants. Alzheimer's Research & Therapy. 2024;16(1):43.
23. Basser PJ, Jones DK. Diffusion-tensor MRI: theory, experimental design and data analysis - a technical review. NMR in biomedicine. 2002;15(7-8):456-67.
24. Kiely M, Triebswetter C, Cortina LE, Gong Z, Alsameen MH, Spencer RG, et al. Insights into human cerebral white matter maturation and degeneration across the adult lifespan. NeuroImage. 2022;247:118727.
25. Deoni SC. Quantitative relaxometry of the brain. Top Magn Reson Imaging. 2010;21(2):101-13.
26. Jiang J, Zhuo Z, Wang A, Li W, Jiang S, Duan Y, et al. Choroid plexus volume as a novel candidate neuroimaging marker of the Alzheimer's continuum. Alzheimer's Research & Therapy. 2024;16(1):149.
27. Ferrucci L. The Baltimore Longitudinal Study of Aging (BLSA): a 50-year-long journey and plans for the future. The journals of gerontology Series A, Biological sciences and medical sciences. 2008;63(12):1416.
28. Shock NW. Normal human aging : the Baltimore longitudinal study of aging. Shock NW, editor. Baltimore, Md: U.S. Dept. of Health and Human Services, Public Health Service, National Institutes of Health, National Institute on Aging, Gerontology Research Center; 1984.
29. O'Brien RJ, Resnick SM, Zonderman AB, Ferrucci L, Crain BJ, Pletnikova O, et al. Neuropathologic studies of the Baltimore Longitudinal Study of Aging (BLSA). J Alzheimers Dis. 2009;18(3):665-75.
30. Bouhrara M, Reiter DA, Celik H, Fishbein KW, Kijowski R, Spencer RG. Analysis of mcDESPOT- and CPMG-derived parameter estimates for two-component nonexchanging systems. Magnetic resonance in medicine. 2016;75(6):2406-20.
31. Bouhrara M, Spencer RG. Incorporation of nonzero echo times in the SPGR and bSSFP signal models used in mcDESPOT. Magnetic resonance in medicine. 2015;74(5):1227-35.
32. Bouhrara M, Spencer RG. Improved determination of the myelin water fraction in human brain using magnetic resonance imaging through Bayesian analysis of mcDESPOT. Neuroimage. 2016;127:456-71.
33. Bouhrara M, Spencer RG. Rapid simultaneous high-resolution mapping of myelin water fraction and relaxation times in human brain using BMC-mcDESPOT. Neuroimage. 2017;147:800-11.
34. Faulkner ME, Gong Z, Guo A, Laporte JP, Bae J, Bouhrara M. Harnessing myelin water fraction as an imaging biomarker of human cerebral aging, neurodegenerative diseases, and risk factors influencing myelination: A review. J Neurochem. 2024.
35. Bouhrara M, Spencer RG. Steady state double angle method for rapid B1 mapping. Magnetic Resonance in Medicine 2018.
36. Kiely M, Triebswetter C, Gong Z, Laporte JP, Faulkner ME, Akhonda M, et al. Evidence of An Association Between Cerebral Blood Flow and Microstructural Integrity in Normative Aging Using a Holistic MRI Approach. J Magn Reson Imaging. 2022.
37. Delis DC, Kramer JH, Kaplan E, Ober BA. California Verbal Learning Test. Assessment. 1987.
38. Reitan R. Trail making test: Manual for administration and scoring: Reitan Neuropsychology Laboratory. Back to cited text. 1992(48).

39. Wechsler D. Wechsler adult intelligence scale. Frontiers in Psychology. 1981.
40. Newcombe F. Missile wounds of the brain: A study of psychological deficits. 1969.
41. Benton AL. Differential behavioral effects in frontal lobe disease. Neuropsychologia. 1968;6(1):53-60.
42. Weston PS, Simpson IJ, Ryan NS, Ourselin S, Fox NC. Diffusion imaging changes in grey matter in Alzheimer's disease: a potential marker of early neurodegeneration. Alzheimers Res Ther. 2015;7(1):47.
43. Vogt NM, Hunt JF, Adluru N, Dean DC, Johnson SC, Asthana S, et al. Cortical Microstructural Alterations in Mild Cognitive Impairment and Alzheimer's Disease Dementia. Cereb Cortex. 2020;30(5):2948-60.
44. Song L, Li Y, Han X, Wang J, Li C, Cong L, et al. Choroid plexus volume, cognitive spectrum, and biomarkers of brain aging in older adults: The MIND-China MRI Study. Alzheimer's & Dementia. 2023;19(e073068).
45. Martinkova JN, Ferretti MT, Ferrari A, Lerch O, Matuskova V, Secnik J, et al. Longitudinal progression of choroid plexus enlargement is associated with female sex, cognitive decline and ApoE E4 homozygote status. Front Psychiatry. 2023;14.
46. Choi JD, Moon Y, Kim HJ, Yim Y, Lee S, Moon WJ. Choroid Plexus Volume and Permeability at Brain MRI within the Alzheimer Disease Clinical Spectrum. Radiology. 2022;304(3):635-45.
47. Jiang J, Zhuo Z, Wang A, Li W, Jiang S, Duan Y, et al. Choroid plexus volume as a novel candidate neuroimaging marker of the Alzheimer's continuum. Alzheimers Res Ther. 2024;16(1):149.
48. Serot JM, Bene MC, Faure GC. Choroid plexus, aging of the brain, and Alzheimer's disease. Front Biosci. 2003;8:s515-21.
49. Marques F, Sousa JC, Brito MA, Pahnke J, Santos C, Correia-Neves M, et al. The choroid plexus in health and in disease: dialogues into and out of the brain. Neurobiol Dis. 2017;107:32-40.
50. Damkier HH, Brown PD, Praetorius J. Cerebrospinal fluid secretion by the choroid plexus. Physiol Rev. 2013;93(4):1847-92.
51. Dani N, Herbst RH, McCabe C, Green GS, Kaiser K, Head JP, et al. A cellular and spatial map of the choroid plexus across brain ventricles and ages. Cell. 2021;184(11):3056-74 e21.
52. Schwartz M, Baruch K. The resolution of neuroinflammation in neurodegeneration: leukocyte recruitment via the choroid plexus. EMBO J. 2014;33(1):7-22.
53. Xu H, Lotfy P, Gelb S, Pragana A, Hehnly C, Byer LIJ, et al. The choroid plexus synergizes with immune cells during neuroinflammation. Cell. 2024;187(18):4946-63 e17.
54. Xu Y, Wang M, Li X, Lu T, Wang Y, Zhang X, et al. Glymphatic dysfunction mediates the influence of choroid plexus enlargement on information processing speed in patients with white matter hyperintensities. Cereb Cortex. 2024;34(6).
55. Municio C, Carrero L, Antequera D, Carro E. Choroid Plexus Aquaporins in CSF Homeostasis and the Glymphatic System: Their Relevance for Alzheimer's Disease. Int J Mol Sci. 2023;24(1).
56. Hong H, Hong L, Luo X, Zeng Q, Li K, Wang S, et al. The relationship between amyloid pathology, cerebral small vessel disease, glymphatic dysfunction, and cognition: a study based on Alzheimer's disease continuum participants. Alzheimers Res Ther. 2024;16(1):43.
57. May C, Kaye JA, Atack JR, Schapiro MB, Friedland RP, Rapoport SI. Cerebrospinal fluid production is reduced in healthy aging. Neurology. 1990;40(3 Pt 1):500-3.
58. Chiu C, Miller MC, Caralopoulos IN, Worden MS, Brinker T, Gordon ZN, et al. Temporal course of cerebrospinal fluid dynamics and amyloid accumulation in the aging rat brain from three to thirty months. Fluids Barriers CNS. 2012;9(1):3.